Real-time Characterization of Cell Membrane Disruption by α-Synuclein Oligomers in Live SH-SY5Y Neuroblastoma Cells

Jacob Parres-Gold[1], Andy Chieng[1], Stephanie Wong Su[1], and Yixian Wang[1]*

[1] Department of Chemistry and Biochemistry, California State University, Los Angeles, Los Angeles, California 90032, United States

Keywords: *α-Synuclein, Parkinson's disease, scanning ion conductance microscopy, membrane disruption, real-time imaging*

ABSTRACT

Aggregation of the natively unfolded protein α-synuclein (α-Syn) has been widely correlated to the neuronal death associated with Parkinson's disease. Mutations and protein overaccumulation can promote the aggregation of α-Syn into oligomers and fibrils. Recent work has suggested that α-Syn oligomers can permeabilize the neuronal membrane, promoting calcium influx and cell death. However, the mechanism of this permeabilization is still uncertain and has yet to be characterized in live cells. This work uses scanning ion conductance microscopy (SICM) to image, in real time and without using chemical probes, the topographies of live SH-SY5Y neuroblastoma cells after exposure to α-Syn oligomers. Substantial morphological changes were observed, with micrometer-scale hills and troughs observed at lower α-Syn concentrations (1.00 μM) and large, transient pores observed at higher α-Syn concentrations (6.0 μM). These findings suggest that α-Syn oligomers may permeabilize the neuronal membrane by destabilizing the lipid bilayer and opening transient pores.

INTRODUCTION

Parkinson's disease (PD) is an increasingly prevalent neurodegenerative disorder characterized by the death of dopamine-producing neurons in the substantia nigra region of the midbrain.[1] Loss of these neurons can impair dopamine-dependent neurological pathways, inducing symptoms of PD such as muscle tremors and cognitive dysfunction.[2] Neuronal death in PD has been widely attributed to the aggregation of the natively unfolded protein α-synuclein (α-Syn).[1] Mutations, protein overaccumulation, posttranslational modifications, and oxidative damage have all been observed to promote the aggregation of monomeric α-Syn into soluble oligomers or fibrils, both containing cores of hydrophobic β-sheets.[3] Recent work has argued that, while fibrils found in clusters known as Lewy bodies are a traditional hallmark of PD, oligomers are the most toxic form of α-Syn.[1] α-Syn oligomers can be secreted from neurons in exosomes, a finding that prompted proposals of prion-like mechanisms for the cell-to-cell transmission of PD.[4,5]

α-Syn oligomers have been observed to induce neuronal death by disrupting a variety of cellular processes, including calcium signaling, the mitochondrial electron transport chain, and the lysosomal autophagy system.[5] Disruption of these processes appears to induce neuronal death while promoting further aggregation of α-Syn. For instance, α-Syn oligomers have been demonstrated to induce irregular calcium influx from the cerebrospinal fluid to the cytoplasm in a manner independent of known calcium transport pathways.[6] The imported calcium has been shown to localize to the mitochondria,[7] at which α-Syn aggregates have been found to independently interfere with complex I-dependent respiration, promoting the production of superoxide.[8] The resulting combination of calcium and superoxide has been proposed to open the mitochondrial permeability transition pore, releasing cytochrome c into the cytoplasm and initiating apoptosis.[9,10] Appropriately, neurons of the substantia nigra are

particularly susceptible to this oxidative stress because they bear a high respiratory demand; these neurons must maintain resting potentials and oscillating calcium concentrations across long axons using active transport.[5,11,12]

A critical step in this proposed sequence of events is the disruption of the neuronal plasma membrane by α-Syn oligomers. Monomers of α-Syn are known to bind negatively charged vesicles with high curvature by adopting α-helical conformations in their N-termini.[13] α-Syn oligomers have also been demonstrated to tightly bind lipid membranes, but with little electrostatic specificity, using a hydrophobic β-sheet core.[14,15] This binding has been observed to increase the permeability of liposomes and supported lipid bilayers to small ions like Ca^{2+} and, to a lesser extent, larger molecules such as glucose, dopamine, and Fura-2.[16,17]

Several mechanisms for membrane permeabilization by α-Syn oligomers have been proposed. Some groups, such as Schmidt et al., have proposed that α-Syn oligomers perforate the membrane with individual protein pores after observing stepwise increases in the conductance of synthetic lipid bilayers treated with α-Syn oligomers.[18] However, other publications have suggested that membrane permeabilization by α-Syn oligomers is less discrete and only occurs after a critical amount of protein has bound the membrane.[19–21] These works have proposed that the binding of α-Syn oligomers to the cell membrane disrupts lipid packing, alters membrane curvature, and extracts lipids from the membrane onto adsorbed aggregates.[21,22] These disruptions would impose tension on the membrane, which – when severe enough – would be expected to open large pores stabilized by α-Syn oligomers at the pore edges[23]; this mechanism is conceptually similar to that by which many antimicrobial peptides permeabilize membranes.[24] Atomic force microscopy (AFM) imaging of supported lipid bilayers and fixed cells in the presence of α-Syn oligomers has suggested the formation of micrometer-scale pores in the membrane, supporting this 'membrane destabilization' model.[25–27]

This work aimed to investigate membrane disruption by α-Syn oligomers in live SH-SY5Y neuroblastoma cells – rather than supported lipid bilayers, liposomes, or fixed cells – in real time. This was done using scanning ion conductance microscopy (SICM), a topographical imaging technique that monitors the electrolytic current flowing through the tip of a nanopipette probe.[28] This current is dependent on the separation between the probe and the sample and thus can be used to map the sample's topography. Significantly, SICM can image the membrane topographies of live neuroblastoma cells in artificial cerebrospinal fluid (ACSF) with nanometer precision, without using chemical probes, in real time. Compared to other topographical imaging techniques, such as AFM, SICM is less likely to damage or distort biological samples throughout imaging because it exerts a negligible force on the sample.[29,30] Additionally, because SICM probes can be cheaply fabricated, newly made probes can be used in each experiment to prevent sample contamination. Thus, this work aimed to use SICM to characterize the mechanism of α-Syn-induced disruption of membranes in live neurons.

RESULTS AND DISCUSSION

To study membrane disruption by α-Syn, aggregates of α-Syn were produced and purified in-vitro. Noncontact air-mode AFM was used to assess the size of the prepared aggregates adhered to a flat mica substrate. Previous work has suggested that, when imaged with AFM, α-Syn oligomers appear as particles with z-heights ranging from 3-16 nm.[3,31] Characterization of the aggregates by AFM determined that the z-heights of the aggregates ranged from 3.50 to 11.00 nm, as shown in Figures 1A and 1B. The arithmetic mean of aggregate z-heights was 5.59 nm (n = 6892), with a 95% confidence interval of (5.53 nm, 5.64 nm). No α-Syn fibrils were observed. Representative AFM images of α-Syn monomers are provided and discussed in the Supporting Information; statistical analysis suggested that the α-Syn oligomers were significantly larger than the α-Syn monomers ($p < 0.001$).

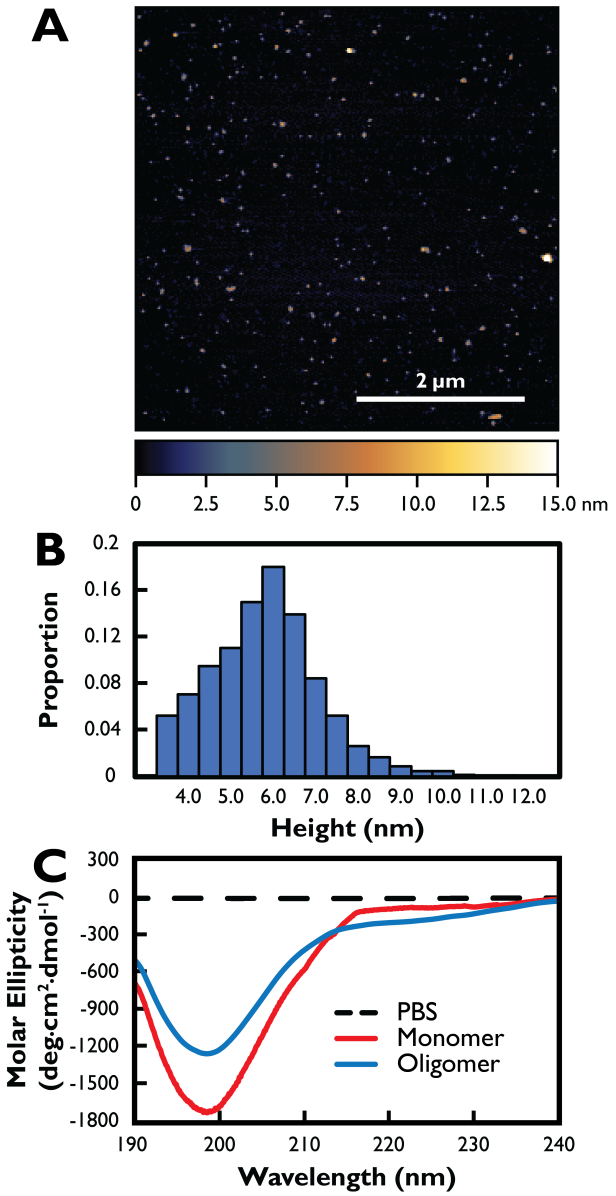

Figure 1. Characterization of α-Syn aggregates. (A) AFM image of α-Syn aggregates adhered to a mica substrate. Pixels are colored by z-height to show aggregate size. Images were first-order flattened using Gwyddion. (B) Histogram of the z-heights of aggregates imaged with AFM (n = 6892). (C) Circular dichroism (CD) spectra of α-Syn aggregates in phosphate buffer (blue line), α-Syn monomers in phosphate buffer (red line), and phosphate buffer alone (black dashed line).

Circular dichroism (CD) spectroscopy was used to investigate the secondary structure of the produced α-Syn aggregates. Previous works have suggested that, while α-Syn monomers exist primarily in the unfolded state or as helical tetramers, α-Syn oligomers and fibrils adopt structures with approximately 35% and 65% β-sheet content, respectively, when measured by CD spectroscopy.[3,31] The CD spectra obtained for monomers and the produced aggregates (Figure 1C) were analyzed using CDPro, suggesting that the α-Syn aggregates had adopted significant β-sheet content (35 ± 7%), in contrast to the α-Syn monomers, which were composed primarily of unfolded content (76 ± 7%, with 8 ± 7% β-sheet content). Thus, the characterization of the α-Syn aggregates by AFM and CD spectroscopy supported the presence of α-Syn oligomers in the aggregate sample.

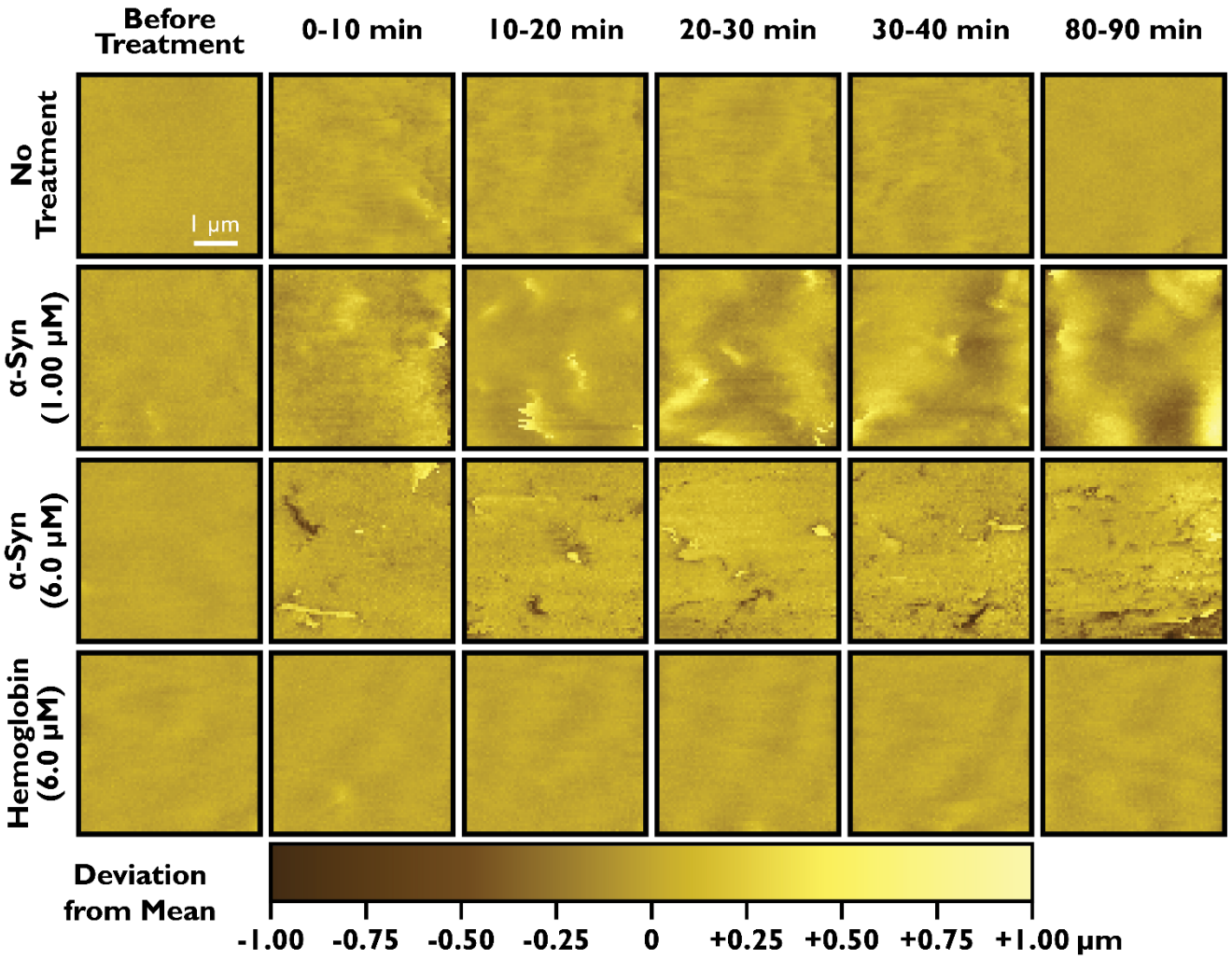

Figure 2. Real-time characterization of cell membrane disruption by SICM. Representative images show flattened maps of 4 × 4 μm sections of the cell membrane, with pixels colored by their deviation from the mean z-height. Selected timepoints are shown for four experimental conditions: No Treatment, α-Syn oligomer treatment (1.00 μM and 6.0 μM), and hemoglobin (negative control, 6.0 μM).

The produced α-Syn oligomers were applied extracellularly to live SH-SY5Y neuroblastoma cells. Previous work has suggested that α-Syn oligomers may partially permeabilize liposomes at concentrations near 0.10-1.00 μM, with maximum permeabilization at higher concentrations (3.0-10.0 μM).[21] Similarly, other works in the literature have observed changes to lipid bilayer curvature at α-Syn concentrations of 0.50-1.00 μM[22] and pore formation at α-Syn concentrations of 2.5-10.0 μM.[19,21,25,26] Thus, in this work, α-Syn oligomers were applied extracellularly at monomer-equivalent concentrations of 1.00 ± 0.03 μM and 6.0 ± 0.2 μM. The topography of the cell membrane was imaged in 10-minute intervals, as shown in Figure 2. To ensure that SICM imaging does not significantly alter the membrane topography, live neurons were imaged in ACSF solution without added protein for over 3 h, showing minimal changes in morphology. Conversely, in the presence of 1.00 μM α-Syn oligomers, large hills and troughs on the order of 2 μm in lateral size and ± 0.5 μm in z-height appeared on the membrane. In the presence of 6.0 μM α-Syn oligomers, curvature changes were still observed, and several large pores appeared in the membrane. These pores were 0.5-1 μm in lateral size and displayed z-heights of -0.4 to -0.8 μm. Additionally, several small features could be observed on the membrane with z-heights ranging from +0.3 to +0.6 μm; line profile plots of these features can be found in the Supporting Information (Figure S3). In both experiments using α-Syn oligomers, the neuroblastoma cells survived for approximately 1.5 h. To confirm that the observed changes

in membrane topography were specifically due to interaction with α-Syn aggregates, neuroblastoma cells were also imaged in the presence of hemoglobin (6.0 μM), a tetrameric globular protein not expected to disrupt neuronal cell membranes. Minimal changes to the membrane topography were observed, suggesting that the presence of micromolar concentrations of protein in the extracellular solution does not nonspecifically alter membrane topography. This finding indicates that the observed membrane disruptions were likely due to membrane binding by α-Syn oligomers.

SICM imaging was also used to investigate the disruption of live neuroblastoma cell membranes by α-Syn monomers. Figure 3 shows representative SICM images of a neuroblastoma cell membrane treated with 2.5 ± 0.08 μM α-Syn monomers. The cells treated with α-Syn monomers survived for approximately 2.5 h. Little disruption was seen in the first 100 min of the experiment, so the α-Syn monomer concentration was increased to 5.0 ± 0.2 μM. Even at this higher concentration, only small curvature changes could be observed after 2 h. These curvature changes were similar in z-height but smaller in lateral size than those observed for 1.00 μM α-Syn oligomers. Additionally, no pores could be observed, in contrast to the images obtained for samples treated with 6.0 μM α-Syn oligomers. These findings support the hypothesis that α-Syn monomers are less able than α-Syn oligomers to permeabilize the cell membrane.[16]

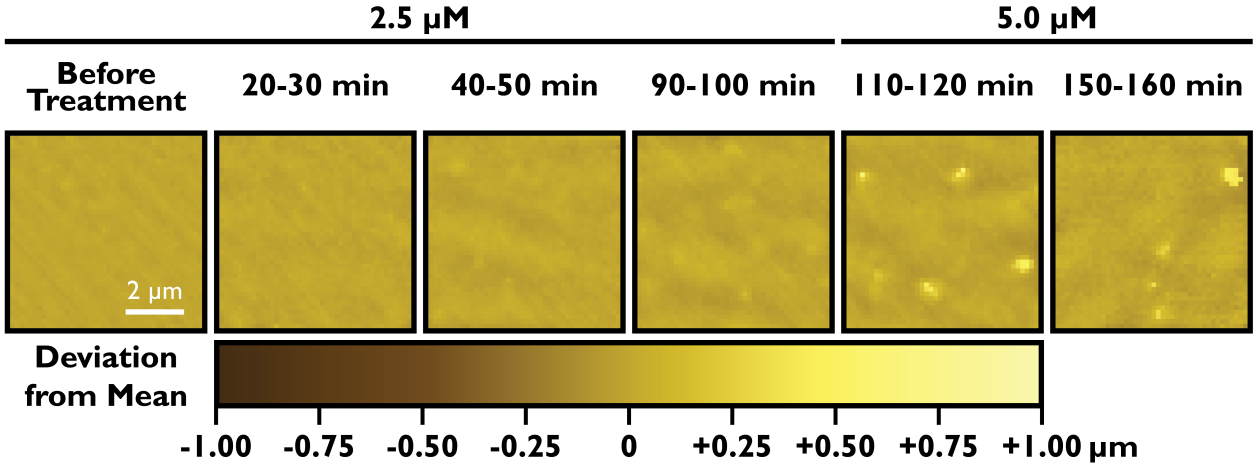

Figure 3. Real-time characterization of cell membrane disruption by α-Syn monomers using SICM. Representative images show flattened maps of 6.5 × 6.5 μm sections of the cell membrane, with pixels colored by their deviation from the mean z-height. Selected timepoints are shown for neuroblastoma cell membranes treated with α-Syn monomers at an initial concentration of 2.5 μM (0-100 min), which was later increased to 5.0 μM (100-160 min).

Changes in membrane topography were quantified by measuring membrane roughness over time, as shown in Figure 4. For neuroblastoma cell membranes imaged without treatment or in the presence of 6.0 μM hemoglobin, roughness remained constant throughout imaging, as normalized roughness values did not significantly exceed 1 ($p > 0.05$). However, the membrane roughness increased significantly after treatment with α-Syn oligomers. At all timepoints, the membrane roughness after treatment with α-Syn oligomers was significantly larger than that of the membrane before treatment ($p < 0.01$). Additionally, at all timepoints other than 90 min, treatment with 6.0 μM α-Syn oligomers gave significantly larger ($p < 0.01$) roughness values than treatment with 1.00 μM α-Syn oligomers and treatment with 2.5 μM α-Syn monomers. After an initial roughness increase, roughness did not appear to continue increasing over time; for samples treated with either 1.00 μM or 6.0 μM α-Syn, none of the post-treatment roughness measurements were significantly different from each other ($p > 0.05$). For samples treated with α-Syn monomers, roughness remained approximately constant (not significantly different from 1, $p > 0.05$) until after 100 min, as the α-Syn concentration was increased to 5.0 μM, when it climbed to approximately 1.5 times the initial value (not shown in Figure 4).

These results provide a wealth of information regarding membrane disruption by α-Syn oligomers in live neuroblastoma cells. At a lower concentration (1.00 μM) of α-Syn, neuronal membranes were significantly distorted, forming large hills and troughs. This finding supports the model suggesting that binding of α-Syn oligomers compresses the outer leaflet of the lipid bilayer, encouraging changes in local membrane curvature, as illustrated in Figure 5. Such micrometer-scale changes have been previously observed at similar concentrations in supported lipid bilayers (0.4 μM α-Syn).[22] At a higher concentration (6.0 μM) of α-Syn, large pores were observed in the membrane. These pores were not static and appeared at different locations at each timepoint; we attribute this observation to the fluidity of the lipid bilayer. These findings support the proposition that higher concentrations of α-Syn oligomers increase tension on the membrane to open transient, micrometer-scale pores, as previously observed at similar concentrations in supported lipid bilayers (2.5 μM α-Syn)[25] and fixed cells (2 μM and 10 μM α-Syn).[26,27] Additionally, several small features were observed to form on the membrane; these features may represent the extraction of membrane lipids to form protein/lipid clusters on the surface of the cell, as previously observed in supported lipid bilayers (3.0 μM α-Syn).[22]

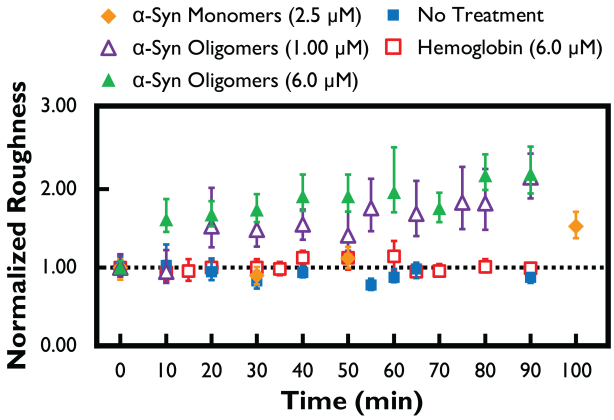

Figure 4. Quantification of cell membrane roughness over time. Roughness was measured for each 1 × 1 μm section of the SICM images by calculating the root-mean-square deviation of z-heights from the mean. Error bars show 95% confidence intervals for the mean calculated by bootstrapping. Data are shown for five experimental conditions: extracellular α-Syn aggregates (1.00 μM, n = 36; 6.0 μM, n = 49), extracellular α-Syn monomers (2.5 μM, n=36), no treatment (n = 36), and extracellular hemoglobin (negative control, 6.0 μM, n = 25). Samples sizes refer to the number of data points for each timepoint.

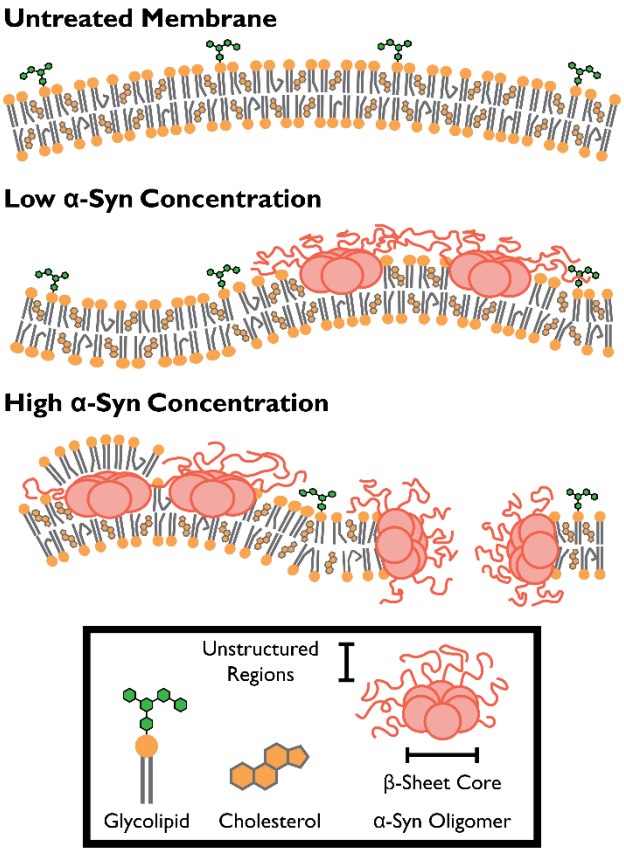

Figure 5. Illustration of the proposed lipid bilayer destabilization model for membrane disruption by α-Syn aggregates. Neuronal membrane proteins have been omitted for clarity. At low concentrations, α-Syn oligomers embed in the membrane using their hydrophobic β-sheet core, disrupting lipid packing and changing membrane curvature. As more α-Syn oligomers embed in the membrane, tension increases until protein-stabilized pores are opened. Lipid extraction also increases membrane tension and forms protein/lipid clusters on the surface of the membrane.

This work has characterized the disruption of live neuronal membranes by α-Syn oligomers applied at two different concentrations. While previous works have investigated the binding and damage of model membranes and fixed cells by α-Syn oligomers, these studies do not account for the complex composition and fluidity of real neuronal membranes, which include many types of phospholipids, glycolipids, and membrane proteins as well as a high proportion of cholesterol. SICM imaging suggested that α-Syn oligomers applied extracellularly may disrupt lipid packing in live cell membranes, altering membrane curvature and even opening large pores in the membrane. However, while α-Syn oligomers are present at low concentrations in the cerebrospinal fluid of PD patients, they primarily occupy the neuronal cytoplasm.[32] Thus, further work is necessary to demonstrate that this work's results apply to disruption by intracellular aggregates. We expect similar results because, although the inner leaflet of the plasma membrane lacks glycolipids and contains a higher proportion of unsaturated phospholipids compared to the outer leaflet,[33] its characteristics do not immediately suggest a reason for a difference in interaction.[34]

Additionally, while α-Syn is N-terminally acetylated in-vivo,[3] this work studied unmodified α-Syn because the membrane permeabilizing activity of unmodified α-Syn has been most widely studied in the literature. This was done to demonstrate that SICM can be reliably used to monitor membrane disruption. Future work is necessary to thoroughly investigate the membrane-disrupting activity of N-terminally acetylated α-Syn.

The large membrane pores described in this work might offer a mechanism for the α-Syn-induced influx of extracellular calcium previously observed in both vesicles[16] and acute rat brain tissue slices.[6] This calcium influx would allow for calcium accumulation in the mitochondria, which – in combination with the oxidative stress created by complex I inhibition by α-Syn – would initiate the opening of the mitochondrial permeability transition pore, promoting the release of cytochrome c and signaling cell death.[10] Future work aims to characterize in more detail the protein-membrane interactions driving membrane binding and disruption as well as the biological consequences of these processes (such as calcium influx, superoxide generation, and cell death). This work will also further explore the interactions of various isoforms of α-synuclein, such as fibrils, epigallocatechin gallate (EGCG)-treated oligomers, and N-terminally acetylated α-synuclein. Such efforts may reveal strategies to prevent or mitigate damage to the neuronal membrane in patients with PD.

METHODS

α-Synuclein Expression, Purification, Aggregation, and Characterization. α-Syn protein was produced in BL21 (DE3) *E. coli* transfected with a pRK172 plasmid containing the wild-type human α-Syn gene originally donated by Prof. Peter Lansbury (Harvard University). α-Syn was aggregated using a protocol adapted from Chen et al.[31] α-Syn (800 μM) was incubated in PBS at 37 °C for 22-24 h. The aggregate sample was filtered through an Amicon Ultra centrifugal filter (100 kDa cutoff, Millipore-Sigma, Burlington, MA) to remove monomers; oligomers were backwashed off the filter with PBS and stored at room temperature for no longer than 14 d.

AFM images were acquired in noncontact air mode with a Park NX12 multifunctional microscopy platform equipped with a detachable AFM head (Park Systems, Seoul, South Korea). The acquired images were linearly flattened and aligned with Gwyddion version 2.51 (http://gwyddion.net/).[35] For characterization by circular dichroism spectroscopy, α-Syn aggregates were diluted to a monomer concentration of 15 μM in 5 mM phosphate buffer (pH 7.40). A J-1100 Circular Dichroism Spectrophotometer (JASCO, Inc., Easton, MD) was used to obtain all measurements. The circular dichroism spectrum obtained for the α-Syn aggregates was compared to those of 56 known proteins with the CONTIN/LL algorithm in CDPro to estimate secondary structure composition.[36] Detailed information regarding the bacterial expression of α-Syn, AFM imaging, and CD spectroscopy can be found in the Supporting Information.

Scanning Ion Conductance Microscopy of Live SH-SY5Y Neuroblastoma Cells. Nanopipette SICM probes were pulled from quartz capillaries to give tip radii of approximately 30-50 nm. The nanopipettes were filled with ACSF solution and fitted with Ag/AgCl electrodes. All images were acquired with a Park NX12 multifunctional microscopy platform (Park Systems) equipped with a detachable SICM head. A CCD camera (Pike F-032B, Allied Vision, Exton, PA) was connected to the optical microscope to assist in probe positioning. SH-SY5Y neuroblastoma cell media was exchanged with ACSF solution warmed to 37 °C. Images were acquired in approach-retract-scan (ARS) mode with a threshold of 0.99 I_0; ARS parameters were varied to optimize image quality without sacrificing imaging speed.

The acquired SICM images were flattened according to a two-dimensional polynomial profile and aligned with Gwyddion version 2.51. Roughness was measured across the membrane surface in 1 μm × 1 μm sections as the root-mean-square deviation of z-heights from the average. Detailed information regarding the SICM imaging, the SICM image processing, and the statistical analysis of roughness measurements can be found in the Supporting Information.

ASSOCIATED CONTENT

Supporting Information

Complete details of the methods and results of this work are provided as supporting information. This includes descriptions of the materials used, the bacterial expression of α-Syn, AFM imaging, CD spectroscopy, the neuroblastoma cell culture, SICM imaging, data processing, and the statistical analysis of roughness measurements as well as SICM line profile plots of the observed membrane pores and simulated SICM approach curves demonstrating the negligible effects of membrane surface charge. This material is available free of charge via the Internet at http://pubs.acs.org.

AUTHOR INFORMATION

Corresponding Author

Yixian Wang, E-mail: ywang184@calstatela.edu, Telephone: +1-323-343-2353.

Department of Chemistry & Biochemistry, California State University, Los Angeles, 5151 State University Drive, Los Angeles, CA 90032

Author Contributions

J.P.-G. prepared the α-Syn aggregates and performed the AFM and CD experiments. J.P.-G. and A.C. performed the SICM experiments and analyzed data. S.W.S. expressed and purified the monomeric α-synuclein. Y.W. is credited with the conceptual design of the project. J.P.-G. prepared the manuscript with the help of A.C. and Y.W. All authors discussed the manuscript and approved the final manuscript submission.

Funding Sources

This work was supported by the California State University Program for Education and Research in Biotechnology (CSUPERB), the California State University, Los Angeles (Cal State LA) Office of Research, Scholarship, and Creative Activities (ORSCA), the Cal State LA Maximizing Access to Research Undergraduate Student Training in Academic Research (MARC USTAR) program (NIH T34GM08228), and the Cal State LA Minority Biomedical Research Support – Research Initiative for Scientific Enhancement (MBRS-RISE) program (NIH R25GM061331). This work was also supported by the National Science Foundation (NSF) Major Research Instrumentation (MRI) grant (NSF 1828334) and the NSF Centers of Research Excellence in Science and Technology Center for Energy and Sustainability (CREST-CEaS, NSF HRD-1547723). The content of this work is solely the responsibility of the authors and does not necessarily represent the official views of the funders.

Notes

The authors declare no competing financial interest.

ACKNOWLEDGMENT

Prof. Feimeng Zhou (California State University, Los Angeles) and his students Xiaoying Wang and Ernest Enriquez are greatly appreciated for sharing their resources and assisting with sample preparation. Prof. Paul Nerenberg (California State University, Los Angeles) is gratefully acknowledged for suggesting methods of statistical analysis. Dev Jasuja is thanked for designing COMSOL simulations to determine the influence of surface charge on SICM imaging.

ABBREVIATIONS

α-Syn, α-synuclein; ACSF, artificial cerebrospinal fluid; AFM, atomic force microscopy; CD, circular dichroism; PD, Parkinson's disease; PBS, phosphate-buffered saline; SICM, scanning ion conductance microscopy

REFERENCES

(1) Stefanis, L. α-Synuclein in Parkinson's disease. *Cold Spring Harb. Perspect. Med.* **2012**, *4*, a009399.

(2) Hamani, C.; Lozano, A. M. Physiology and pathophysiology of Parkinson's disease. *Ann. N. Y. Acad. Sci.* **2003**, *991*, 15–21.

(3) Cremades, N.; Chen, S. W.; Dobson, C. M. Structural characteristics of α-synuclein oligomers. *Int. Rev. Cell Mol. Biol.* **2017**, *329*, 79–143.

(4) Emmanouilidou, E.; Melachroinou, K.; Roumeliotis, T.; Garbis, S. D.; Ntzouni, M.; Margaritis, L. H.; Stefanis, L.; Vekrellis, K. Cell-produced α-synuclein is secreted in a calcium-dependent manner by exosomes and impacts neuronal survival. *J. Neurosci.* **2010**, *30* (20), 6838–6851.

(5) Kim, S. D.; Allen, N. E.; Canning, C. G.; Fung, V. S. C. Parkinson disease. *Handb. Clin. Neurol.* **2017**, *3*, 17013.

(6) Angelova, P. R.; Ludtmann, M. H. R.; Horrocks, M. H.; Negoda, A.; Cremades, N.; Klenerman, D.; Dobson, C. M.; Wood, N. W.; Pavlov, E. V.; Gandhi, S.; Abramov, A. Y. Calcium is a key factor in α-synuclein-induced neurotoxicity. *J. Cell Sci.* **2016**, *129* (9), 1792–1801.

(7) Melachroinou, K.; Xilouri, M.; Emmanouilidou, E.; Masgrau, R.; Papazafiri, P.; Stefanis, L.; Vekrellis, K. Deregulation of calcium homeostasis mediates secreted α-synuclein-induced neurotoxicity. *Neurobiol. Aging* **2013**, *34* (12), 2853–2865.

(8) Ludtmann, M. H. R.; Angelova, P. R.; Horrocks, M. H.; Choi, M. L.; Rodrigues, M.; Baev, A. Y.; Berezhnov, A. V.; Yao, Z.; Little, D.; Banushi, B.; Al-Menhali, A. S.; Ranasinghe, R. T.; Whiten, D. R.; Yapom, R.; Dolt, K. S.; Devine, M. J.; Gissen, P.; Kunath, T.; Jaganjac, M.; Pavlov, E. V.; Klenerman, D.; Abramov, A. Y.; Gandhi, S. α-Synuclein oligomers interact with ATP synthase and open the permeability transition pore in Parkinson's disease. *Nat. Commun.* **2018**, *9* (1), 2293–2309.

(9) Rocha, E. M.; De Miranda, B.; Sanders, L. H. α-Synuclein: pathology, mitochondrial dysfunction and neuroinflammation in Parkinson's disease. *Neurobiol. Dis.* **2018**, *109*, 249–257.

(10) Luth, E. S.; Stavrovskaya, I. G.; Bartels, T.; Kristal, B. S.; Selkoe, D. J. Soluble, prefibrillar α-synuclein oligomers promote complex I-dependent, Ca^{2+}-induced mitochondrial dysfunction. *J. Biol. Chem.* **2014**, *289* (31), 21490–21507.

(11) James Surmeier, D.; Guzman, J. N.; Sanchez, J.; Schumacker, P. T. Physiological phenotype and vulnerability in Parkinson's disease. *Cold Spring Harb. Perspect. Med.* **2012**, *2* (7), 1–27.

(12) Calì, T.; Ottolini, D.; Brini, M. Calcium signaling in Parkinson's disease. *J. Cell Tissue Res.* **2014**, *357*, 439–454.

(13) Pirc, K.; Ulrih, N. P. α-Synuclein interactions with phospholipid model membranes: key roles for electrostatic interactions and lipid-bilayer structure. *Biochim. Biophys. Acta, Biomembr.* **2015**, *1848* (10), 2002–2012.

(14) Volles, M. J.; Lee, S. J.; Rochet, J. C.; Shtilerman, M. D.; Ding, T. T.; Kessler, J. C.; Lansbury, P. T. Vesicle permeabilization by protofibrillar α-synuclein: implications for the pathogenesis and treatment of Parkinson's disease. *Biochemistry* **2001**, *40* (26), 7812–7819.

(15) Fusco, G.; Chen, S. W.; Williamson, P. T. F.; Cascella, R.; Perni, M.; Jarvis, J. A.; Cecchi, C.; Vendruscolo, M.; Chiti, F.; Cremades, N.; Ying, L.; Dobson, C. M.; De Simone, A. Structural basis of membrane disruption and cellular toxicity by α-synuclein oligomers. *Science* **2017**, *358* (6369), 1440–1443.

(16) Volles, M. J.; Lansbury, P. T. Vesicle permeabilization by protofibrillar α-synuclein is sensitive to Parkinson's disease-linked mutations and occurs by a pore-like mechanism. *Biochemistry* **2002**, *41*, 4595–4602.

(17) Pacheco, C. R.; Morales, C. N.; Ramírez, A. E.; Muñoz, F. J.; Gallegos, S. S.; Caviedes, P. A.; Aguayo, L. G.; Opazo, C. M. Extracellular α-synuclein alters synaptic transmission in brain neurons by perforating the neuronal plasma membrane. *J. Neurochem.* **2015**, *132* (6), 731–741.

(18) Schmidt, F.; Levin, J.; Kamp, F.; Kretzschmar, H.; Giese, A.; Bötzel, K. Single-channel electrophysiology reveals a distinct and uniform pore complex formed by α-synuclein oligomers in lipid membranes. *PLoS One* **2012**, *7* (8), 1–7.

(19) Lorenzen, N.; Nielsen, S. B.; Yoshimura, Y.; Vad, B. S.; Andersen, C. B.; Betzer, C.; Kaspersen, J. D.; Christiansen, G.; Pedersen, J. S.; Jensen, P. H.; Mulder, F. A. A.; Otzen, D. E. How epigallocatechin gallate can inhibit α-synuclein oligomer toxicity in vitro. *J. Biol. Chem.* **2014**, *289* (31), 21299–21310.

(20) van Rooijen, B. D.; Claessens, M. M. A. E.; Subramaniam, V. Membrane permeabilization by oligomeric α-synuclein: in search of the mechanism. *PLoS One* **2010**, *5* (12), 1–9.

(21) Rooijen, B. D. Van; Claessens, M. M. A. E.; Subramaniam, V. Lipid bilayer disruption by oligomeric α-synuclein depends on bilayer charge and accessibility of the hydrophobic core. *Biochim. Biophys. Acta, Biomembr.* **2009**, *1788* (6), 1271–1278.

(22) Reynolds, N. P.; Soragni, A.; Rabe, M.; Verdes, D.; Liverani, E.; Handschin, S.; Riek, R.; Seeger, S. Mechanism of membrane interaction and disruption by α-synuclein. *J. Am. Chem. Soc.* **2011**, *133* (48), 19366–19375.

(23) Ghio, S.; Kamp, F.; Cauchi, R.; Giese, A.; Vassallo, N. Interaction of α-synuclein with biomembranes in Parkinson's disease – role of cardiolipin. *Prog. Lipid Res.* **2016**, *61*, 73–82.

(24) Lee, M. T.; Chen, F. Y.; Huang, H. W. Energetics of pore formation induced by membrane active peptides.

Biochemistry **2004**, *43* (12), 3590–3599.
(25) Chaudhary, H.; Iyer, A.; Subramaniam, V.; Claessens, M. M. A. E. α-Synuclein oligomers stabilize pre-existing defects in supported bilayers and propagate membrane damage in a fractal-like pattern. *Langmuir* **2016**, *32* (45), 11827–11836.
(26) Kumar, R.; Kumari, R.; Kumar, S.; Jangir, D. K.; Maiti, T. K. Extracellular α-synuclein disrupts membrane nanostructure and promotes S-nitrosylation-induced neuronal cell death. *Biomacromolecules* **2018**, *19* (4), 1118–1129.
(27) Wong Su, S.; Chieng, A.; Parres-Gold, J.; Chang, M.; Wang, Y. Real-time determination of aggregated α-synuclein induced membrane disruption at neuroblastoma cells using scanning ion conductance microscopy. *Faraday Discuss.* **2018**, *210*, 131–143.
(28) Hansma, P. K.; Drake, B.; Marti, O.; Gould, S. A. C.; Prater, C. B. The scanning ion-conductance microscope. *Science* **1989**, *243* (4891), 641–643.
(29) Happel, P.; Thatenhorst, D.; Dietzel, I. D. Scanning ion conductance microscopy for studying biological samples. *Sensors* **2012**, *12* (11), 14983–15008.
(30) Seifert, J.; Rheinlaender, J.; Novak, P.; Korchev, Y. E.; Schäffer, T. E. Comparison of atomic force microscopy and scanning ion conductance microscopy for live cell imaging. *Langmuir* **2015**, *31* (24), 6807–6813.
(31) Chen, S. W.; Drakulic, S.; Deas, E.; Ouberai, M.; Aprile, F. A.; Arranz, R.; Ness, S.; Roodveldt, C.; Guilliams, T.; De-Genst, E. J.; Klenerman, D.; Wood, N. W.; Knowles, T. P. J.; Alfonso, C.; Rivas, G.; Abramov, A. Y.; Valpuesta, J. M.; Dobson, C. M.; Cremades, N. Structural characterization of toxic oligomers that are kinetically trapped during α-synuclein fibril formation. *Proc. Natl. Acad. Sci.* **2015**, *112* (16), E1994–E2003.
(32) Gao, L.; Tang, H.; Nie, K.; Wang, L.; Zhao, J.; Gan, R.; Huang, J.; Zhu, R.; Feng, S.; Duan, Z.; Zhang, Y.; Wang, L. Cerebrospinal fluid α-synuclein as a biomarker for Parkinson's disease diagnosis: a systematic review and meta-analysis. *Int. J. Neurosci.* **2015**, *125* (9), 645–654.
(33) Ingólfsson, H. I.; Carpenter, T. S.; Bhatia, H.; Bremer, P. T.; Marrink, S. J.; Lightstone, F. C. Computational lipidomics of the neuronal plasma membrane. *Biophys. J.* **2017**, *113* (10), 2271–2280.
(34) Feng, L. R.; Federoff, H. J.; Vicini, S.; Maguire-Zeiss, K. A. α-Synuclein mediates alterations in membrane conductance: a potential role for a-synuclein oligomers in cell vulnerability. *Eur. J. Neurosci.* **2010**, *32* (1), 10–17.
(35) Nečas, D.; Klapetek, P. Gwyddion: an open-source software for SPM data analysis. *Cent. Eur. J. Phys.* **2012**, *10* (1), 181–188.
(36) Sreerama, N.; Woody, R. W. Estimation of protein secondary structure from circular dichroism spectra: comparison of CONTIN, SELCON, and CDSSTR methods with an expanded reference set. *Anal. Biochem.* **2000**, *287* (2), 252–260.

TABLE OF CONTENTS (TOC) / ABSTRACT GRAPHIC